Journal of Civil Structural Health Monitoring (2024) 14:67–82
https://doi.org/10.1007/s13349-023-00699-0

ORIGINAL PAPER

A novel methodology based on the reflected L(0,1) guided wave for quantitative detection of corrosion-induced wall thickness loss in continuous pipes

Yang Liu[1] · **Xin Feng**[1]

Received: 22 August 2022 / Accepted: 9 April 2023 / Published online: 24 April 2023

Abstract
Corrosion-induced wall thickness loss (CIWTL) can reduce the strength and integrity of a pipe, threatening its normal operation. Effective detection of CIWTL in pipes helps ensure their safe operation. This paper presents a novel methodology based on the reflected L(0,1) guided wave to quantitatively detect CIWTL in a continuous pipe. Investigating the effects of CIWTL and propagation length on time-of-flight (TOF) variation of the L(0,1) guided wave showed that increasing the accumulated propagation length of the L(0,1) mode improved its sensitivity to CIWTL. The reflected L(0,1) guided wave, which had a longer accumulated propagation length in a certain range, was generated by making discontinuities on both sides of a localized section within a continuous pipe. Then, the TOF variation of the reflected wave was proposed as a CIWTL-sensitive feature, and a quantitative relationship between the TOF variation of the reflected wave and CIWTL was theoretically established for quantifying the CIWTL of the pipe section. High-resolution measurement of CIWTL could be achieved through increased accumulated propagation length. Additionally, this methodology could be applied to measure CIWTL in the next pipe section and extended to realize the distributed detection of CIWTL in a continuous pipe. The effectiveness of this methodology was validated experimentally. The experimental results indicated that the L(0,1) mode was clearly reflected from artificial discontinuities, CIWTL in the pipe was sensitively identified and accurately quantified using the proposed method, and the values of the CIWTL measured by the proposed method were consistent with those measured by ultrasonic testing (UT). This methodology has higher estimation performance for CIWTL than current guided wave-based (GWB) methods.

Keywords Continuous pipe · Corrosion-induced wall thickness loss (CIWTL) · Quantitative detection · Reflected L(0,1) guided wave · Time-of-flight (TOF) variation

1 Introduction

Pipes are widely used to transport water, oil, gas, chemical raw materials, and other resources. The operating conditions of pipes are complex and severe [1–3], and they are usually located in humid and corrosive environments. Hence, pipes are susceptible to various types of corrosion, such as localized corrosion and general corrosion [4–7]. The effects of the corrosive media inside and outside the pipe, as well as scouring by high speed flow in the pipe, cause the pipe to undergo general corrosion, which induces thinning of the wall thickness. Corrosion-induced wall thickness loss (CIWTL) can degrade the strength and bearing capacity of a pipe, shorten its service life, and even cause failure. It is therefore vital to quantitatively detect CIWTL of pipes to effectively evaluate their integrity and remaining service life, ensure safe operation, and avoid catastrophic failures. The initiation and propagation of pipe corrosion is a long-term dynamic process. Corrosion accumulates as the service time of the pipe increases. Under the influence of complex factors, the corrosion rate may be accelerated and result in sudden corrosion failure of pipe before routine inspection. Pipes are usually long, and they are inaccessible in some parts. Thus, there is an urgent need for a detection technique with high resolution and the ability to precisely quantify CIWTL and rapidly and comprehensively detect corrosion of an entire pipe.

✉ Xin Feng
fengxin@dlut.edu.cn

[1] Faculty of Infrastructure Engineering, Dalian University of Technology, Dalian, China

Ultrasonic testing (UT) [8] is one of the main conventional nondestructive testing (NDT) methods used to inspect corrosion in pipes, and it has high resolution and precision for wall thickness measurement. Ultrasound has strong ability to penetrate and can perform in-depth inspection of a pipe without affecting its performance. Accordingly, pipe inspection gages based on UT sensors have been developed. They can be inserted into a pipe to inspect corrosion over a long distance during operation of the pipe [9, 10]. Unfortunately, this method is a pointwise inspection technique and requires scanning the pipe wall point by point, which implies low detection efficiency. Additionally, it is impossible to perform this method in hidden and inaccessible portions of a pipe; therefore, it is not suitable for complete coverage of long-distance pipes. UT has demanding requirements for testing conditions; for instance, if the coupling effect between the ultrasonic probe and the surface of the pipe is poor or there are many corrosion pits and deposits of sediment, the inspection precision is greatly reduced. Eddy current, magnetic flux leakage, X-ray, and other conventional techniques are also widely used for corrosion inspection, but they all have defects similar to UT [11–13]. It is difficult to use these conventional methods to effectively detect CIWTL in pipes.

The guided wave-based (GWB) technique is an attractive alternative to conventional pointwise inspection methods and has been proven to be successful in detecting different types of damage in various structures, e.g., corrosion in plates [14, 15], damage to beams [16, 17], localized and general corrosion of steel bars [18, 19], and damage to pipes [20–23]. The GWB technique uses piezoelectric transducers to excite an ultrasonic guided wave in a structure, and the guided wave propagates along the structure. When the guided wave encounters corrosion defects, it undergoes reflection, transmission, mode conversion, and other behaviors. By receiving and analyzing guided wave signals (that contain corrosion defect information) at a remote position, structural corrosion damage can be actively identified. Ultrasonic guided waves can propagate long distances along an entire pipe with low attenuation, and damage over long distances along the pipe can be detected using a single transmitting-receiving device mounted on the surface of the pipe. Additionally, guided waves are capable of quickly and comprehensively interrogating the full cross section of long-distance pipes, including physically inaccessible areas [24–28]. These characteristics enable the GWB technique to comprehensively and effectively detect corrosion of long-distance pipe structures and perform distributed monitoring.

Various GWB methods have been proposed for damage detection of pipes. Lowe et al. [29] and Carandente et al. [30] used the reflection coefficients of incident L(0,2) and T(0,1) modes, respectively, to estimate defect sizes in pipes. The appearance of defect reflections indicated the presence of defects in pipes. There was a correlation between the reflection coefficient and defect size in a pipe, and this correlation was used to qualitatively evaluate the defect size. Wang et al. [31] proposed using the reflection coefficient of symmetric modes converted by incident longitudinal modes to characterize defects, and the results indicated that the converted symmetric modes could provide important information about defects. Ennaceur et al. [32] evaluated defects in pipes using time-reversed technology. The experimental results showed that time-reversed technology could improve the amplitudes of defect reflections, thereby increasing the sensitivity to defects. Amjad et al. [33] calculated the time-of-flight (TOF) of transmitted wave modes to assess the diameter of circular defects in a pipe. The experimental results indicated that the TOF of the transmitted wave increased with increasing diameter of the circular defect. Guan et al. [34] applied nonlinear guided waves to detect fatigue cracks in pipes, proposed using the second harmonic wave generated by micro-cracks to identify fatigue cracks, and introduced a nonlinear index to evaluate the severity of fatigue cracks. The proposed method was verified by an experiment. Available studies have confirmed that signal strength, TOF, nonlinear parameters, and other indexes can identify pipe defects. However, these methods are mainly capable of providing a qualitative evaluation of the degree of damage of the pipe, i.e., slight, moderate and severe. The physical mechanism of the influence of corrosion depth on the evaluation indexes has not been sufficiently clarified on the basis of a theoretical model, and the quantitative relationship between the evaluation indexes and depth of corrosion in a pipe has not yet been theoretically developed; thus, the CIWTL of a pipe cannot be quantified accurately. Additionally, these methods have weak capability for evaluation of small losses of wall thickness, and their stability and repeatability have certain deficiencies. These considerations motivate the development of the GWB approach to quantitatively detect CIWTL in pipes in this study.

In practical projects, continuous pipes are widely used except when segmented pipes are used. For continuous pipes, it is difficult to exploit end reflections due to the limited propagation range of guided waves. In this study, we proposed a novel detection methodology for sensitive identification and accurate quantification of CIWTL in a continuous pipe based on the reflected L(0,1) guided wave. We studied the influences of CIWTL and propagation length on TOF variation of the L(0,1) guided wave in the selected dispersion range and found that increasing the accumulated propagation length of the L(0,1) guided wave could increase its sensitivity to CIWTL. Based on the mechanism of a guided wave in a discontinuous medium, we generated the reflected L(0,1) guided wave by making discontinuities on both sides of local pipe section within the continuous pipe. The change in TOF of the reflected L(0,1) guided wave with respect to the wall thickness was

extracted as a CIWTL-sensitive feature. The quantitative relationship between the TOF variation of the reflected wave and CIWTL was further established theoretically to quantify the CIWTL of the pipe section. The reflected L(0,1) guided wave increased the accumulated propagation length within a certain range, thereby achieving high-resolution measurement of minor corrosion. Then, this proposed methodology could be used to detect CIWTL in the next pipe section. By repeating this process, the CIWTL of a continuous pipe could be detected in a large-scale and distributed manner. An experiment was performed to verify the effectiveness of the proposed methodology. The results showed that the L(0,1) mode was clearly reflected from artificial discontinuities, and this methodology was sensitive to minor corrosion and accurately quantified the CIWTL of the pipe.

2 Detection principle

2.1 Propagation characteristics of guided waves in pipes

A guided wave generated in a pipe by lead zirconate titanate (PZT) transducers propagates along the pipe, and the wall thickness variation caused by corrosion leads to a change in its propagation characteristics. Therefore, the corrosion damage of the pipe can be identified by detecting the change in the ultrasonic guided wave signal. The equation of motion of cylindrical guided waves propagating in a pipe satisfies the Navier's displacement equation:

$$\mu\nabla^2 u + (\lambda+\mu)\nabla(\nabla\cdot u) = \rho\frac{\partial^2 u}{\partial t^2} \tag{1}$$

where μ and λ are the Lamé constants of the material; ∇^2 is the Laplace operator; ρ is the density of the pipe; and u and t are the displacement and time, respectively.

According to the derivation of the displacement solution of Eq. (1) by Gazis [35], solving the displacement of the cylindrical guided wave ultimately reduces to solving the dispersion equation of the cylindrical guided wave in the pipe, namely

$$\left|C_{ij}\right| = 0 \tag{2}$$

where C_{ij} is a 6×6 matrix, $i,j = 1,2,3,4,5,6$; C_{ij} is related to the Lamé constants μ and λ, the density ρ, inner radius a and outer radius b of pipe, and other parameters [35].

The solution of Eq. (2) includes three types of guided wave modes: longitudinal guided wave, torsional guided wave and flexural guided wave. The guided wave mode can be represented by dispersion curves of the group velocity and the phase velocity of the guided wave, and the relationship between them is [36]:

$$C_g = C_p^2\left[C_p - (fd)\frac{dC_p}{d(fd)}\right]^{-1} \tag{3}$$

where $C_g = d\omega/dk$ and $C_p = \omega/k$ are the group velocity and phase velocity, respectively, k and ω are wavenumber and circular frequency, respectively; $f=\omega/2\pi$ is frequency; and d is the wall thickness of the pipe. Equations (2, 3) indicate that the group velocity C_g of the guided wave in the pipe is a function of the wall thickness d of the pipe and the frequency f of the guided wave. The dispersion curves of the guided waves are calculated using the Disperse program [37] to numerically solve Eq. (2). Figure 1 illustrates the group velocity dispersion curves for a steel pipe with 60 mm outer diameter and 7 mm wall thickness.

One of the keys of the GWB technique is to select and exploit a single mode. In general, when the guided wave is dispersive, its group velocity depends on the product of frequency and thickness of the pipe in which it is propagating. As illustrated in Fig. 1, the group velocity of the torsional mode T(0,1) is insensitive to the change in wall thickness since it is nondispersive. Although the flexural modes are dispersive, they have high attenuation. Moreover, the flexural modes are various, their acoustic fields are complex, and the wave velocities of these flexural modes are close, which causes modal aliasing. The L(0,2) guided wave is dispersive in the range of approximately 32.63–60 kHz, indicating that the group velocity of the L(0,2) guided wave in this range is dependent on the product of frequency and thickness. Unfortunately, in this range, the L(0,1) guided wave is present along with the L(0,2) guided wave at a given frequency, which easily causes modal interference and makes signal interpretation difficult. In the whole frequency range, the L(0,1) guided wave is dispersive, so its group velocity

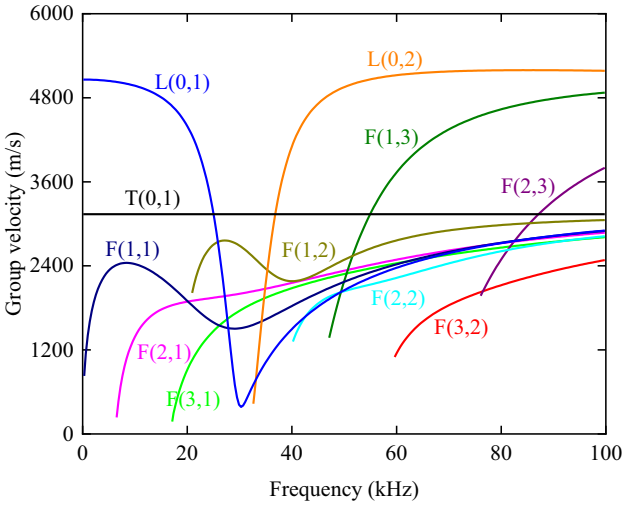

Fig. 1 Group velocity dispersion curves in a pipe

is affected by the wall thickness variation. The longitudinal guided waves are easily excited and controlled, and the attenuations are small during the propagation process. When the excitation frequency is less than the cutoff frequency of the L(0,2) guided wave, a pure L(0,1) guided wave can be excited, which facilitates signal analysis. As mentioned above, the L(0,1) guided wave was selected to detect the CIWTL of a pipe. CIWTL in a pipe changes the group velocity of the L(0,1) guided wave at a constant frequency and thus changes the TOF of the L(0,1) guided wave. Therefore, the CIWTL of the pipe can be detected by analyzing the TOF variation of the L(0,1) guided wave.

2.2 TOF variation of L(0,1) guided wave caused by CIWTL

To accurately quantify the CIWTL of a pipe, it is necessary to further investigate the effect of CIWTL on the propagation characteristics of the L(0,1) guided wave in theory to extract CIWTL-sensitive features and establish a quantitative relationship between a sensitive feature and CIWTL. Figure 2 depicts the group velocity curves of the L(0,1) guided wave generated for various wall thicknesses ranging from 7 to 5 mm. In the frequency range of approximately 0–30 kHz, the group velocity of the L(0,1) guided wave at a constant frequency decreases as the wall thickness decreases. Therefore, the TOF of the L(0,1) guided wave at a constant frequency increases with increasing CIWTL in the pipe. To investigate the relationship between group velocity variation and frequency, the group velocity variations caused by wall thickness loss of 0.5 mm at different frequencies were obtained by subtracting the group velocity curve for the wall thickness of 7 mm from that for the wall thickness of 6.5 mm. As illustrated in Fig. 3, in the frequency range of 0–28.05 kHz, the change in group velocity increases as the frequency increases. In the frequency range of 28.05–30 kHz, the higher the frequency is, the smaller the change in group velocity. The frequency of 28.05 kHz is most sensitive to the change in wall thickness. Hence, to more effectively detect CIWTL in a pipe, the excitation signal with a central frequency close to 28.05 kHz should be selected as far as possible under the condition that it can excite a pure L(0,1) guided wave and receive a pure L(0,1) guided wave with clear amplitude.

To simulate the influence of corrosion on group velocity, the initial inner radius a_h of the pipe and the inner radius a_c of the pipe after corrosion were substituted into Eq. (2). The group velocity curves corresponding to the initial wall thickness d_h of the pipe and the wall thickness d_c of the pipe after corrosion were generated, and then the corresponding group velocities C_{gh} and C_{gc} were obtained at the constant frequency f_o, respectively. The expressions for the CIWTL of the pipe and the corresponding TOF variation of the L(0,1) guided wave are as follows:

$$\left.\begin{aligned} \Delta d &= a_c - a_h = d_h - d_c \\ \Delta t &= t_c - t_h = L\left(\frac{1}{C_{gc}} - \frac{1}{C_{gh}}\right) \end{aligned}\right\} \tag{4}$$

where Δd and Δt are the CIWTL of the pipe and the corresponding TOF variation of the L(0,1) guided wave, respectively; t_h and t_c are the TOF of the L(0,1) guided wave before and after corrosion, respectively; and L is the propagation length of the L(0,1) guided wave.

Equation (4) shows that the TOF variation Δt of the L(0,1) guided wave can be used to assess the CIWTL Δd of

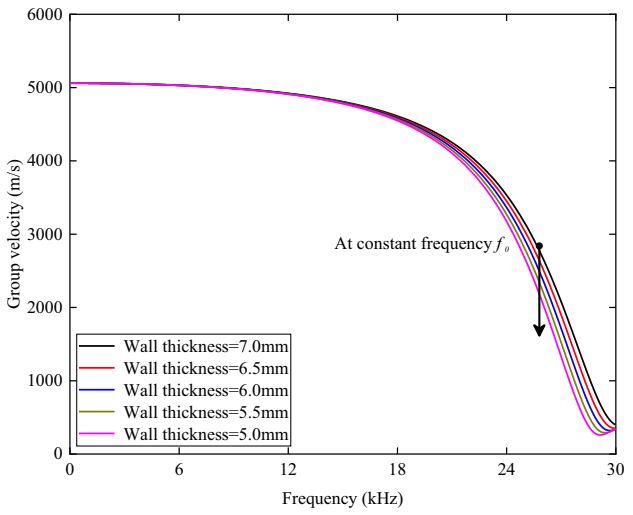

Fig. 2 Group velocity dispersion curves of L(0,1) guided waves for different wall thicknesses

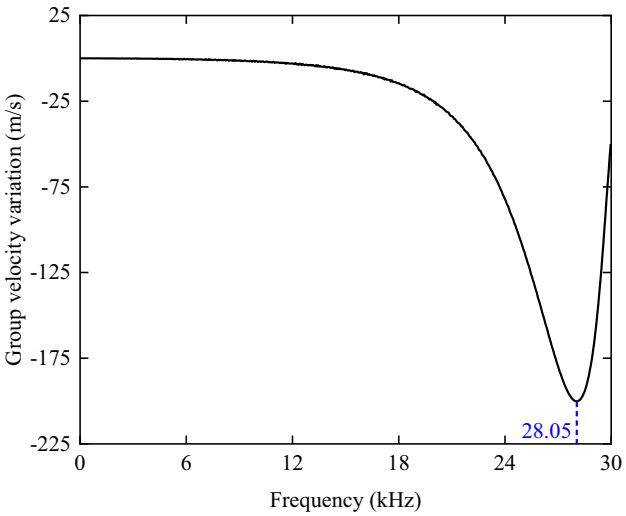

Fig. 3 Group velocity variation curve of the L(0,1) guided wave

the pipe. By calculating the TOF variations corresponding to different CIWTLs, the relationship curve between the TOF variation and the CIWTL was established. Taking the frequency of 25 kHz and the reduction in wall thickness from 7 mm to 5.4 mm as an example, the quantitative relationship curves of TOF variation and CIWTL were established theoretically when the propagation lengths were 1, 2 and 3 m, respectively. Figure 4 illustrates that under the conditions of a constant frequency f_o and a certain propagation length, the TOF variation Δt was positively associated with the CIWTL. The explicit quantitative relationship between the TOF variation and CIWTL was used to quantify the CIWTL of the pipe. Moreover, at a constant frequency f_o and a certain wall thickness loss Δd_0, the TOF variation Δt was proportional to the propagation length of guided wave.

Equation (4) and Fig. 4 show that the measurement precision of the TOF variation determines the resolution and quantification precision for the CIWTL. In practice, however, due to the influences of random and systematic errors, there is some uncertainty in the measurement of TOF variation. When the TOF variation of the L(0,1) guided wave caused by corrosion is small, the precision of the measured TOF variation is low, resulting in low precision for the quantification of CIWTL in the pipe. Therefore, to sensitively identify minor corrosion and accurately quantify CIWTL in the pipe, it was necessary to increase the TOF variation caused by corrosion as much as possible. At a constant frequency f_o and a certain corrosion degree Δd_0, the TOF variation mainly depends on the propagation length L. Thus, a longer propagation length was needed to obtain a larger TOF variation. The propagation length of the direct wave is the distance between the transmitting and receiving transducers. For a given pipe, the distance between the transmitting and receiving transducers is constant. At a constant excitation frequency, the resolution and quantification precision of the TOF variation of the direct wave to the CIWTL of the pipe were determined. Using the TOF variation of the direct wave to detect the CIWTL of the pipe may have low resolution and quantification precision, which is easy to cause misjudgment of corrosion and has certain limitations.

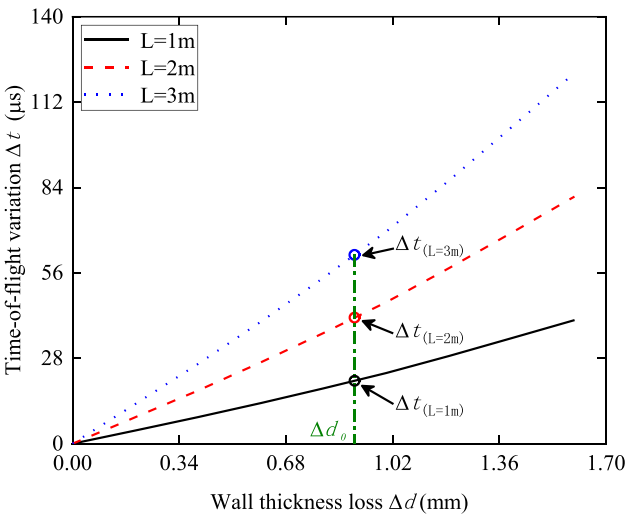

Fig. 4 Quantitative relationships between TOF variation and CIWTL

2.3 CIWTL detection based on the reflected L(0,1) guided wave for a continuous pipe

The reflected wave propagates back and forth in a pipe, which can significantly increase its accumulated propagation length in a certain range. Reflected waves are generated when the incident guided wave encounters discontinuities in the structures [25, 38, 39]. Significantly, the L(0,1) guided wave is the axisymmetric longitudinal mode, and the generated reflected waves contain only the axisymmetric longitudinal modes, provided that these axisymmetric longitudinal modes act on axisymmetric structural features in a pipe, such as flanges [40, 41]. Thus, a pure L(0,1) mode can be reflected from axisymmetric structures, while the L(0,1) guided wave with frequencies less than the cutoff frequency of an L(0,2) guided wave is excited in the pipe. However, in comparison with the whole length of continuous pipe, the propagation length of the L(0,1) guided wave is very limited because of the attenuation of the stress wave and confined energy of the actuator. Thus, the challenge was how to create the reflected L(0,1) guided wave in the localized section within the continuous pipe. Based on the mechanism of a guided wave in a discontinuous medium, we proposed a novel method to detect the CIWTL of a continuous pipe based on the reflected L(0,1) guided wave. The approach involved two parts: (1) a detection scheme for generating the reflected L(0,1) guided wave in a continuous pipe and (2) a quantitative algorithm for detecting CIWTL.

The CIWTL detection scheme for a continuous pipe is shown in Fig. 5. First, the transmitting and receiving arrays are installed at the positions of interest on the continuous pipe, and the pipe section with a certain length containing the transmitting and receiving arrays is selected as the measurement section. The distance between the transmitting array and the left side of the pipe section is equal to the distance between the receiving array and the right side of the pipe section. Two identical metal rings are bonded on both sides of the pipe section using epoxy resin, thereby creating artificial discontinuous impedances and forming axisymmetric structural features in the continuous pipe. Second, the L(0,1) guided wave whose frequencies are less than the cutoff frequency of the L(0,2) guided wave is selected as the excitation signal to act on the pipe, and the L(0,1) mode can be reflected from the metal rings. Under the conditions that the reflected wave generated at the metal rings can be separated from the reflection signals from other places in the continuous pipe and the clear reflected

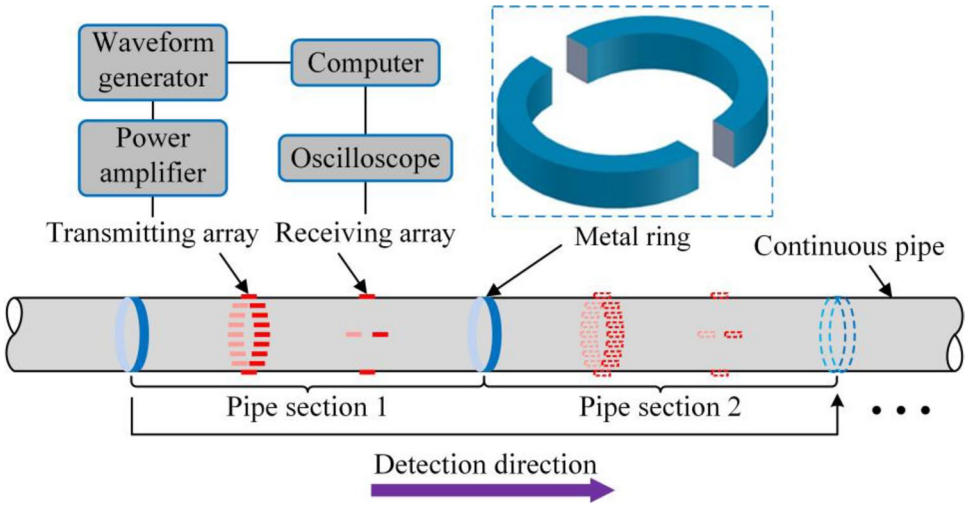

Fig. 5 CIWTL detection scheme for a continuous pipe

wave can be received, the reflected L(0,1) guided wave traversing the pipe section between the two metal rings as many times as possible can be used. A longer propagation length is used to obtain higher sensitivity and quantification precision for CIWTL. Third, the TOF variation of the reflected L(0,1) guided wave is calculated to quantitatively identify the CIWTL of this pipe section. Finally, after the CIWTL detection of the pipe section is completed, along the pipe detection direction, the metal ring far away from the next pipe section can be disassembled and bonded on the other side of the next pipe section, and the CIWTL of the next pipe section can be detected. Therefore, the CIWTL of different pipe sections i ($i = 1, 2, 3, \ldots, n$) can be detected separately, and large-scale and distributed detection of the CIWTL in a continuous pipe can be realized. Each metal ring is composed of two identical metal semirings, which is convenient for bonding, ensures excellent coupling between the metal ring and the surface of the pipe and enables the metal ring to be disassembled and reused.

The propagation length of the reflected wave is larger than that of the direct wave, which can significantly improve the resolution and quantification precision for the CIWTL of the pipe section. In pipe section i, the TOF variations of the direct wave and the reflected wave under the same wall thickness loss can be written as:

$$\left.\begin{aligned}\Delta t_{d_i} &= t_{(dc)_i} - t_{(dh)_i} = L_{d_i}\left(\frac{1}{C_{(gc)_i}} - \frac{1}{C_{(gh)_i}}\right)\\ \Delta t_{r_i} &= t_{(rc)_i} - t_{(rh)_i} = L_{r_i}\left(\frac{1}{C_{(gc)_i}} - \frac{1}{C_{(gh)_i}}\right)\end{aligned}\right\} \tag{5}$$

where Δt_{d_i} and Δt_{r_i} are the TOF variations of the direct wave and the reflected wave corresponding to pipe section i, respectively; $t_{(dh)_i}$ and $t_{(dc)_i}$ are the TOFs of the direct wave when pipe section i is in an intact state and subjected to corrosion, respectively; $t_{(rh)_i}$ and $t_{(rc)_i}$ are the TOFs of the reflected wave when pipe section i is in an intact state and subjected to corrosion, respectively; L_{d_i} and L_{r_i} are the propagation lengths of the direct wave and the reflected wave corresponding to pipe section i, respectively; and $C_{(gh)_i}$ and $C_{(gc)_i}$ are the group velocities of the L(0,1) guided wave at constant frequency f_o when pipe section i is in an intact state and subjected to corrosion, respectively.

With the use of Eq. (5), under the same wall thickness loss, when the propagation length of the reflected wave is m times that of the direct wave (i.e., $L_{r_i} = mL_{d_i}$), the TOF variation of the reflected wave is m times that of the direct wave. Therefore, the resolution of the TOF variation of the reflected wave to the CIWTL of pipe section i is m times that of the TOF variation of the direct wave to the CIWTL of pipe section i. The TOF variation of the reflected wave is larger than that of the direct wave and has higher quantification precision for the CIWTL of pipe section i. The TOF variation of the reflected wave is therefore proposed as a CIWTL-sensitive feature to identify the CIWTL of pipe section i. At the constant frequency f_o and the propagation length L_{r_i} of the reflected wave, the quantitative relationship between the TOF variation of the reflected wave and the CIWTL of pipe section i is established theoretically to quantitatively evaluate the CIWTL of pipe section i. The value of the CIWTL of pipe section i is further deduced using the TOF variation of the reflected wave extracted from the measured guided wave signals and the quantitative relationship to effectively detect the CIWTL of pipe section i. Each pipe section can be quantified using this method separately, and thus the CIWTL of a continuous pipe can be quantified in a distributed manner. To reduce the impact of noise and accurately extract the TOF of the guided wave at the central frequency, continuous wavelet transform (CWT) technology [42] is used to perform time–frequency analysis on the received guided waves. The TOF corresponding to the maximum value of the wavelet coefficient at the center frequency

is extracted, and the TOF variations of reflected wave under different corrosion degrees are obtained.

3 Experimental investigations

An experiment was performed to validate the effectiveness of the proposed methodology. The experimental setup is depicted in Fig. 6. The experimental carbon steel pipe had a length of 5.06 m, an outer diameter of 60 mm, and a wall thickness of 7 mm. PZT transducers with a size of 25 × 4 × 1 mm were used as transmitters and receivers. The transmitting array was composed of 16 PZTs with equal circumferential spacing, and the receiving array was composed of 4 PZTs with equal circumferential spacing; all the PZTs were bonded on the pipe using epoxy resin. The transmitting array and the receiving array were 2.055 m and 3.005 m from the left end of the pipe, respectively. All the transmitters were connected in parallel, and they were excited equally and simultaneously. Each receiver individually received guided wave signals. The guided wave signals received by each receiver mainly contained the information about the corrosion depth on the axial path of the pipe where the receiver was located. The receivers were numbered PZT1, PZT2, PZT3 and PZT4, and the corresponding axial detection paths of the pipe were path1, path2, path3 and path4, respectively. Two identical metal rings were symmetrically installed on the pipe to make discontinuities and form axisymmetric structural features, thus generating reflected waves in the pipe. The 20-cycle sine wave modulated by a Hanning window was used as the excitation signal, and a narrower bandwidth was selected to minimize the signal attenuation caused by dispersion. Based on the investigation of frequency selection in Sect. 2.2, the center frequency of the excitation signal was preliminarily limited to the range of 23–27 kHz. According to the calculated theoretical wave velocities corresponding to these frequencies and the length of the pipe, it could be roughly judged that the reflected wave generated at the metal rings could be effectively separated from both direct wave and end reflection signals when the distance between the two metal rings was approximately within 2.8–3.2 m. Thus, to obtain better sensitivity and quantification precision for CIWTL, these two metal rings were bonded on the pipe 1.055 m from the left of the transmitting array and 1.055 m from the right of the receiving array using epoxy resin. Notably, we only received the first reflected L(0,1) guided wave from the metal rings due to the limitation of the length of the experimental pipe. Guided waves usually propagate tens of meters. In practical applications, with a certain distance between the two metal rings, the reflected L(0,1) guided wave traversing the pipe section between the two metal rings as many times as possible can be used under the conditions proposed in the second step of the detection scheme in Sect. 2.3. Thus, higher resolution and quantification precision for CIWTL can be obtained.

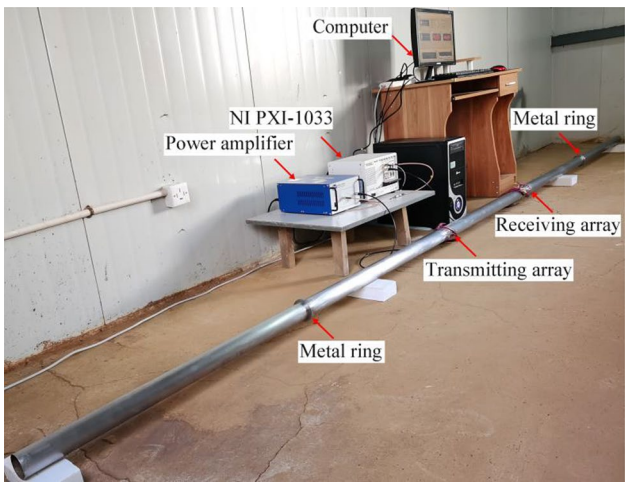

Fig. 6 Experimental setup

The waveforms generated by the arbitrary waveform generator card (PXI-5421) were amplified by the power amplifier (Trek 2100HF) and then sent to the transmitting array to excite the guided wave signal in the pipe. The oscilloscope card (PXI-5122) was connected to each receiver to record the guided wave signals independently. The sampling frequency was 4 MHz, and the sampling time was 2 ms to ensure that the direct wave and the reflected wave signals were completely acquired. The PXI-5421 and PXI-5122 cards were included in the National Instruments (NI) PXI-1033 chassis. A computer with a LabVIEW program was used for setting the excitation signal, data acquisition, and synchronization control in the experiment. Figure 7 shows the fabricated metal rings. Each metal ring was made of steel and had a height of 15 mm, an outer diameter of 80 mm, and a wall thickness of 10 mm.

To select the appropriate center frequency, we set the center frequencies as 23, 24, 25, 26, and 27 kHz. According to the initial guided wave signals received in the experiment, when the center frequency was 25 kHz, the received L(0,1) guided waves had large amplitudes and clear modes. Additionally, all wave packets were effectively separated, and there was no modal interference. Therefore, it was easy to analyze the received signals and extract the TOF of each wave packet. When the center frequency exceeded 25 kHz, the signals had obvious attenuations and gradual waveform distortions, and other modes gradually appeared, which resulted in modal aliasing. A 20-cycle 25 kHz sine wave modulated by a Hanning window was thus used as the excitation signal. The transmitters were length expander-types, and their number was sufficient; thus, only the longitudinal modes were excited. The frequencies contained in the excitation signal were less than the cutoff frequency of the

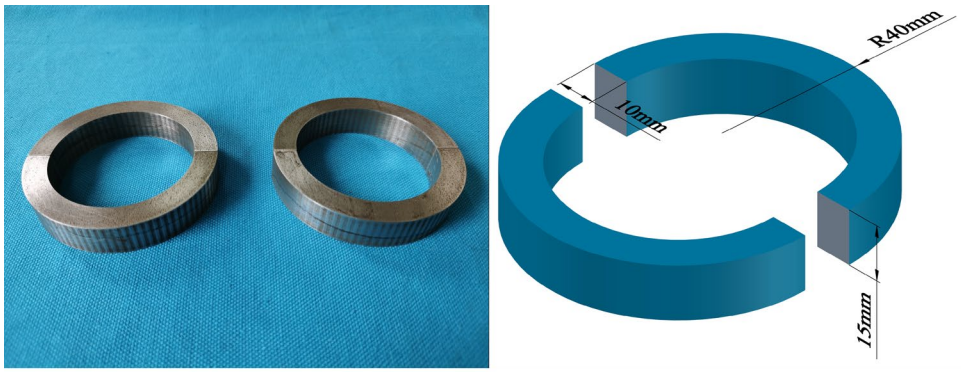

(a) (b)

Fig. 7 Fabricated metal rings

L(0,2) guided wave, the peak frequency of each wave packet was almost 25 kHz, and its corresponding group velocity was consistent with the group velocity corresponding to the L(0,1) guided wave. This confirmed that all measured wave packets were L(0,1) modes.

To simulate the CIWTL of the pipe, the experimental steel pipe was subjected to accelerated corrosion tests using the impressed direct-current (DC) technique. A stainless steel pipe with a length of 5.5 m, an outer diameter of 20 mm, and a wall thickness of 1 mm was centered inside the pipe along its axis. The stainless steel pipe was connected to the cathode, and the experimental carbon steel pipe was connected to the anode. Each end of the pipe was sealed by attaching a piece of plexiglass plate using epoxy resin. A plastic pipe was used to connect one end of the pipe to a bucket filled with 3.5% NaCl solution, and a pump was used to fill the inside of the steel pipe with NaCl solution. The other plastic pipe was used to connect the other end of the pipe to the bucket to discharge the gas and corrosion products induced by corrosion. A DC power supply was used to impress a DC to accelerate the corrosion of the pipe. The value of the current was set at 18 A, and the corresponding current density was small, approximately 2.46 mA/cm^2. In each case of corrosion, the left and right sides of the pipe were alternately used as the input end of the current, and the corrosion test was conducted for the same length of time. Thus, the difference in corrosion rates between the two sides of the pipe was minimized, and the inner wall of the pipe corroded uniformly. The accelerated corrosion tests continued for 470 h. The CIWTL of the pipe was detected after 140, 200, 327 and 470 h of corrosion. Figure 8 illustrates the details of the accelerated corrosion device, and Fig. 9 shows the diagram of different degrees of corrosion.

The steel pipe was cleaned and dried before each data acquisition. Values of the CIWTL of the pipe were obtained using an ultrasonic thickness gage (Olympus MG2-DL) to measure the wall thicknesses of the steel pipe before and after corrosion. Figure 10 illustrates the wall thickness measurement of the pipe. Starting at 1.44 m from the left end of the pipe, 6 equally spaced (i.e., 0.44 m) points for measuring the wall thickness were set on each detection path of the outer surface of the pipe. The average value of the wall thicknesses at 6 measuring points was calculated as the average wall thickness of the corresponding detection path. In all corrosion cases, the wall thickness loss of each path was acquired by subtracting the average wall thickness of the path in the corrosion case from the initial average value. The wall thickness losses of 4 paths under different corrosion cases are tabulated in Table 1. These results indicated that the inner wall of the pipe was underwent relatively uniform corrosion throughout the process.

4 Experimental results and discussion

4.1 Analysis of guided wave signals

The guided wave signals received by the four PZTs were almost the same. Figure 11 shows the guided wave signal of PZT1 at the baseline and corresponding CWT. As expected, each guided wave signal contained two complete wave packets; the first wave packet was the direct wave, whereas the second wave packet was the reflected wave generated at the metal rings. The received guided wave signal was explicitly separated into two wave packets through CWT, which had high time–frequency resolution. The propagation lengths of the two wave packets are depicted in Fig. 12. The propagation lengths of the direct wave and the reflected wave were 0.95 and 3.06 m, respectively. The propagation length of the reflected wave was approximately 3.22 times that of the direct wave. According to Eq. (5), theoretically, the resolution of the TOF variation of the reflected wave to the CIWTL of the pipe was 3.22 times that of the direct wave. The calculated TOF of the second wave packet was 3.27 times that of the first wave packet, which was in good agreement with theory.

Figure 13 shows the guided wave signals of PZT1 at the baseline and different corrosion times. The guided wave

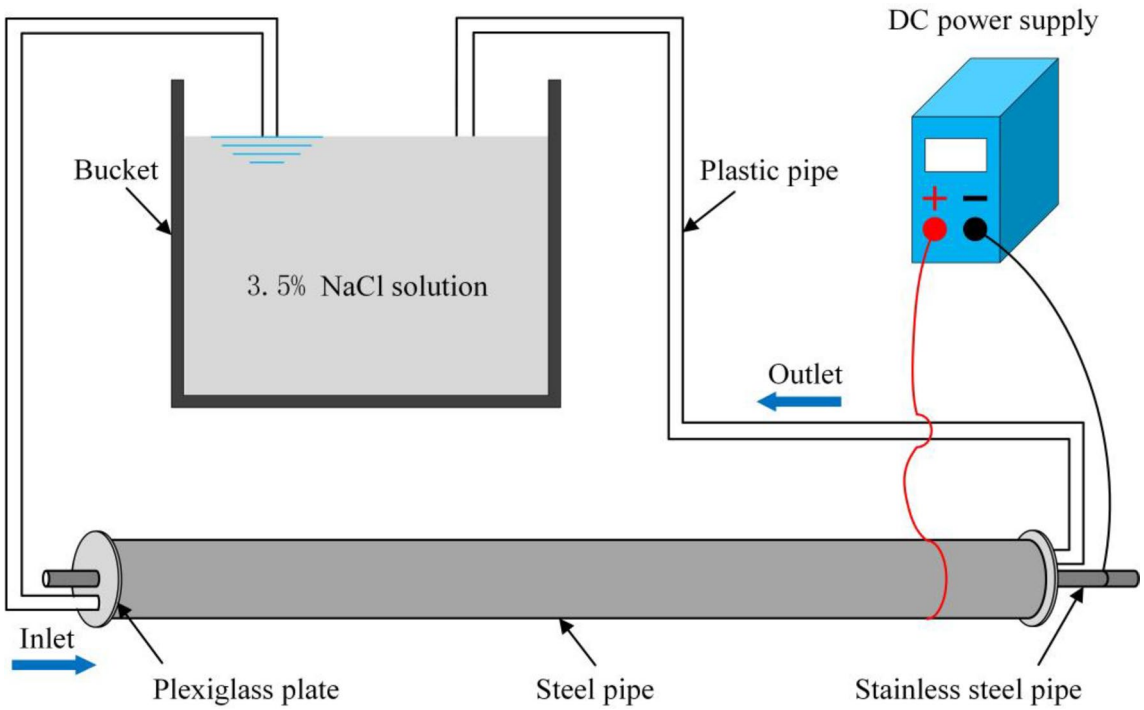

Fig. 8 Accelerated corrosion device

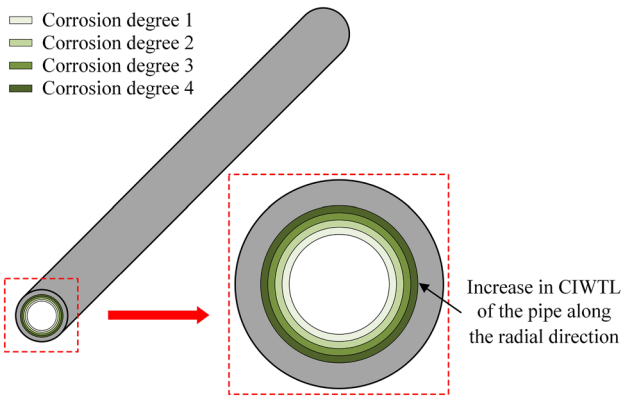

Fig. 9 Diagram of different degrees of corrosion

signals gradually shifted to the right with increasing corrosion time; the amplitudes of guided waves showed slight fluctuations during the whole corrosion process. These observations were attributed to variations in the propagation characteristics of guided waves. Corrosion leads to the gradual thinning of the wall thickness of the pipe, which changes the propagation characteristics of the guided wave and gradually reduces the group wave velocity of the guided wave. As a result, the TOFs of the received guided wave signals gradually increase, and the amplitudes change. During the whole corrosion process, the frequency of each peak was basically always maintained at 25 kHz, and the received guided wave modes remained constant. When the corrosion degree was small, the TOF of the direct wave did not change

Fig. 10 Wall thickness measurement of the pipe

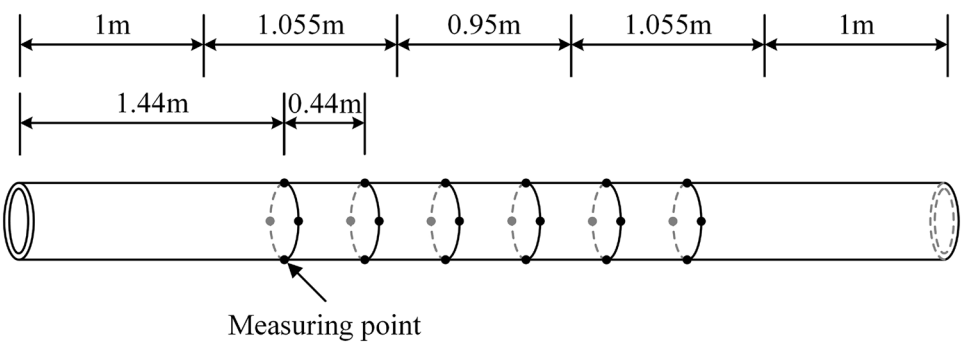

Table 1 Wall thickness losses of 4 paths of the pipe

Path	Wall thickness Losses	Corrosion time (hour)			
		140	200	327	470
1	Δ*d*/mm	0.31	0.50	0.82	1.14
2	Δ*d*/mm	0.34	0.48	0.75	1.09
3	Δ*d*/mm	0.33	0.53	0.86	1.20
4	Δ*d*/mm	0.27	0.49	0.77	1.14

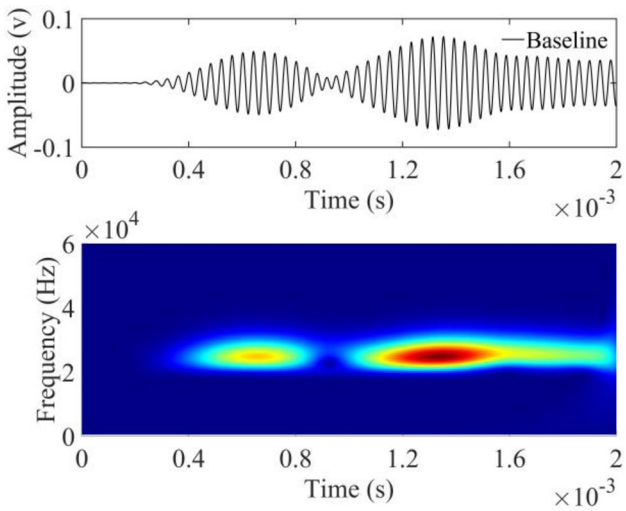

Fig. 11 Guided wave signal of PZT1 at the baseline and corresponding CWT

significantly, whereas the TOF of the reflected wave changed greatly. At the same corrosion degree, the TOF variation of the reflected wave was much greater than that of the direct wave, which indicated that the reflected wave was more sensitive than the direct wave to corrosion. The variations in guided wave signals qualitatively evaluated the corrosion of a pipe. The reflected wave signals provided more accurate information about propagation of corrosion, which could be more effective in detecting the CIWTL of the pipe.

4.2 Quantitative estimation of the CIWTL of the pipe

The CIWTL in a pipe can be qualitatively identified only by analyzing the variation trends of the reflected waves. To accurately quantify the CIWTL in a pipe, the quantitative relationship curves between the TOF variation of the direct wave and the CIWTL for each path and between the TOF variation of the reflected wave and the CIWTL for each path were established theoretically based on the analysis in Sect. 2. The CIWTL of the pipe was quantitatively estimated using the TOF variations of the direct waves and the reflected waves extracted from the measured guided wave signals and these quantitative relationship curves.

As illustrated in Fig. 14, the TOF variations of the direct waves corresponding to the four paths generally showed an increasing trend with increasing corrosion degree, but there were some fluctuations. Furthermore, there were some cases in which the deviations between the measured TOF variations of the direct waves and the corresponding theoretical TOF variations were large, which resulted in the inability to distinguish different CIWTLs. These results indicated that although the TOF variation of the direct wave can evaluate the CIWTL to a certain extent, it was insufficiently sensitive to the CIWTL of the pipe; this was likely to cause misjudgment and could not sensitively identify and accurately quantify the CIWTL of the pipe. Figure 15 shows that the TOF variation of the reflected wave was very sensitive to the CIWTL of the pipe. After one instance of corrosion, the wall thickness losses of the four paths were slight, and the TOF variations of the reflected waves corresponding to the four paths changed significantly. The TOF variation of the reflected wave corresponding to each path was relatively consistent with the corresponding theoretical TOF variation,

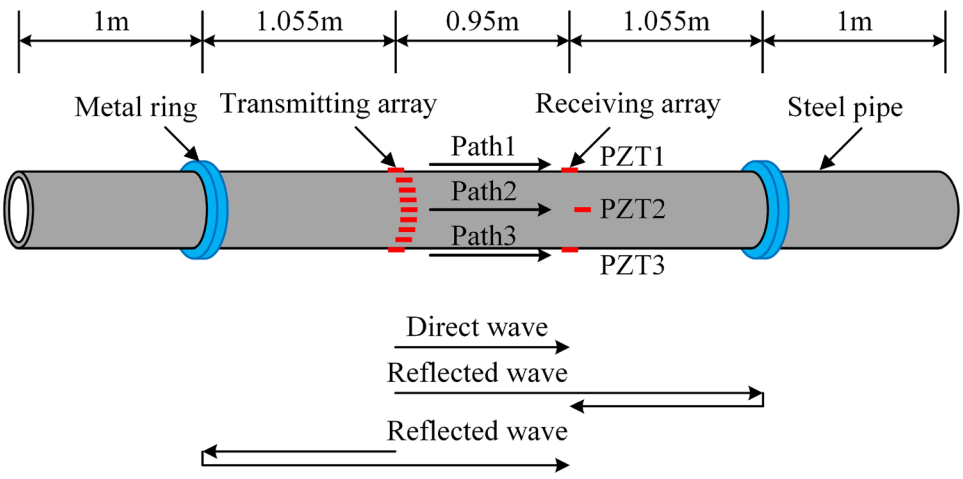

Fig. 12 Diagram of the propagation lengths of the guided waves

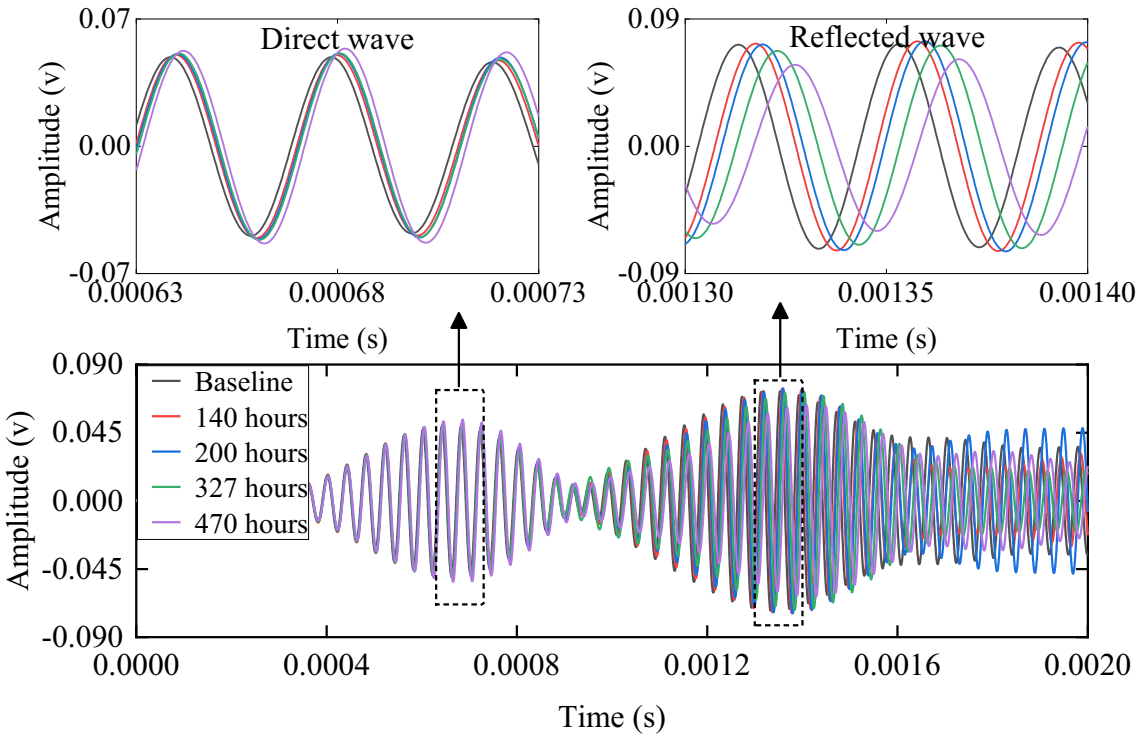

Fig. 13 Guided wave signals received by PZT1 at the baseline and different corrosion times

indicating that the TOF variation of the reflected wave could sensitively identify and accurately quantify minor loss of wall thickness. The TOF variation of the reflected wave in each path increased gradually as the corrosion degree increased. The TOF variations of the reflected waves corresponding to the four paths were in agreement with the corresponding theoretical TOF variations. Therefore, the CIWTL of each path was effectively quantified using the TOF variation of the reflected wave corresponding to that path. At the same corrosion degree, the TOF variation of the reflected wave corresponding to the same path was significantly larger than that of the direct wave, indicating that the TOF variation of the reflected wave was more sensitive than the direct wave to the CIWTL. These results demonstrated that the TOF variation of the reflected wave could be used to sensitively identify and accurately quantify the CIWTL of the pipe.

The CIWTLs measured by the TOF variations of the direct waves were deduced by combining the TOF variations of the direct waves calculated in the experiment and the quantitative relationship between the TOF variation of the direct wave and the CIWTL for each path. Likewise, the CIWTLs measured by the proposed method were deduced by combining the TOF variations of the reflected waves calculated in the experiment and the quantitative relationship between the TOF variation of the reflected wave and the CIWTL for each path. These values measured by the TOF variations of the direct waves and the proposed method were compared with the corresponding values measured by UT.

The wall thicknesses measured by UT showed that for the same corrosion case, there was little difference in the wall thickness losses at all measuring points on the same axial path, and the corresponding standard deviation was small. The CIWTLs of the four paths measured by the TOF variations of the direct waves and those measured by UT are shown in Fig. 16. With increasing corrosion time, the CIWTLs of the four paths measured by the TOF variations of the direct waves fluctuated, although the overall trends increased. Moreover, there were some cases in which the relative errors between the values measured by the TOF variations of the direct waves and the corresponding values measured by UT were large. Therefore, the precision of the CIWTLs of the four paths measured by the TOF variations of the direct waves were insufficient, and the CIWTL of the pipe was not effectively detected. Figure 17 illustrates the CIWTLs of four paths measured by the proposed method and measured by UT. After 140 h of corrosion, the CIWTL of each path of the pipe was slight. The values measured by UT were 0.31, 0.34, 0.33, and 0.27 mm, and the standard deviations were 0.026, 0.023, 0.028, and 0.015 mm, respectively; the values measured by the proposed method were 0.323, 0.377, 0.364, and 0.243 mm. The results showed that the discreteness of wall thickness losses of all measuring points on the same path was small. The relative errors between

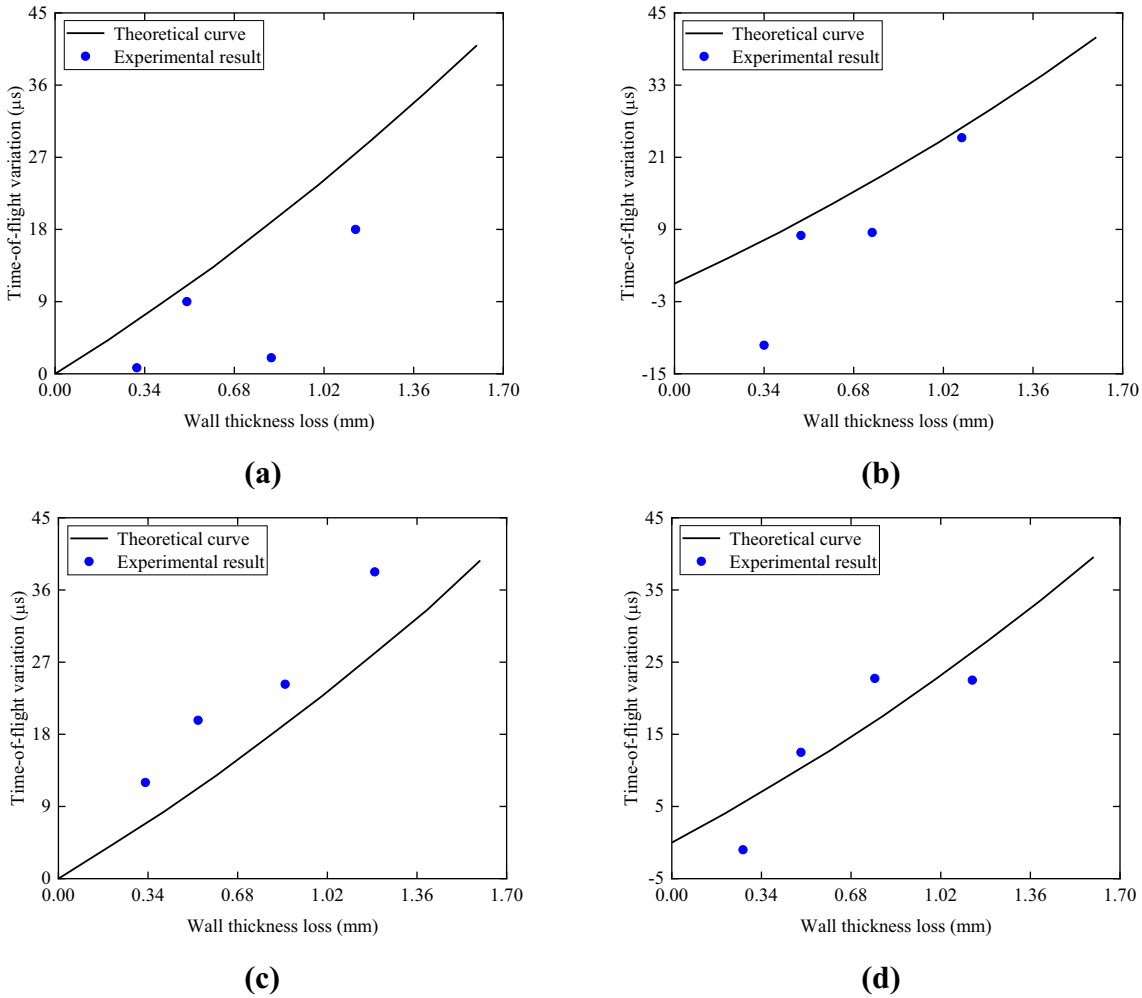

Fig. 14 Time-of-flight variations of the direct waves with different wall thickness losses: **a** path1, **b** path2, **c** path3, and **d** path4

the values measured by the proposed method and the corresponding values measured by UT were small, which indicated that the proposed methodology was sensitive to minor wall thickness loss, had high resolution for the CIWTL, and accurately quantified CIWTL values as small as 0.27 mm. The CIWTLs of the four paths of the pipe measured by the proposed method gradually increased as the corrosion time increased, and there were no fluctuations. After 470 h of corrosion, the CIWTLs of the four paths were severe and exceeded 15% of the initial wall thickness. The values measured by UT were 1.14, 1.09, 1.20 and 1.14 mm, and the standard deviations were 0.032, 0.05, 0.031, and 0.067 mm, respectively; the values measured by the proposed method were 1.007, 0.96, 1.057 and 1.01 mm. Therefore, the fluctuations of wall thickness losses at all measuring points on the same path were small, and there was still good agreement between the values measured by the proposed method and those measured by UT. During the whole corrosion process, the values measured by the proposed method were relatively consistent with those measured by UT, and the maximum error was -11.93%. These results demonstrated that the proposed methodology had not only high quantification precision and a large detection range for the CIWTL of the pipe but also good stability and feasibility. However, evaluation indexes, such as signal strength and nonlinear parameters, are easily perturbed by external factors, such as bonding conditions between transducers and pipe, noise, and so forth, and it is difficult to guarantee stability and repeatability. The corrosion of each path for the pipe was comprehensively detected using the deployed receiver network.

The experimental results showed that the CIWTL of the pipe was effectively identified and quantified using the first reflected L(0,1) guided wave signal. In practical applications, the reflected L(0,1) guided wave traversing the pipe section between the two metal rings as many times as possible can be used under the conditions proposed in the second step of the detection scheme in Sect. 2.3. Thus, the

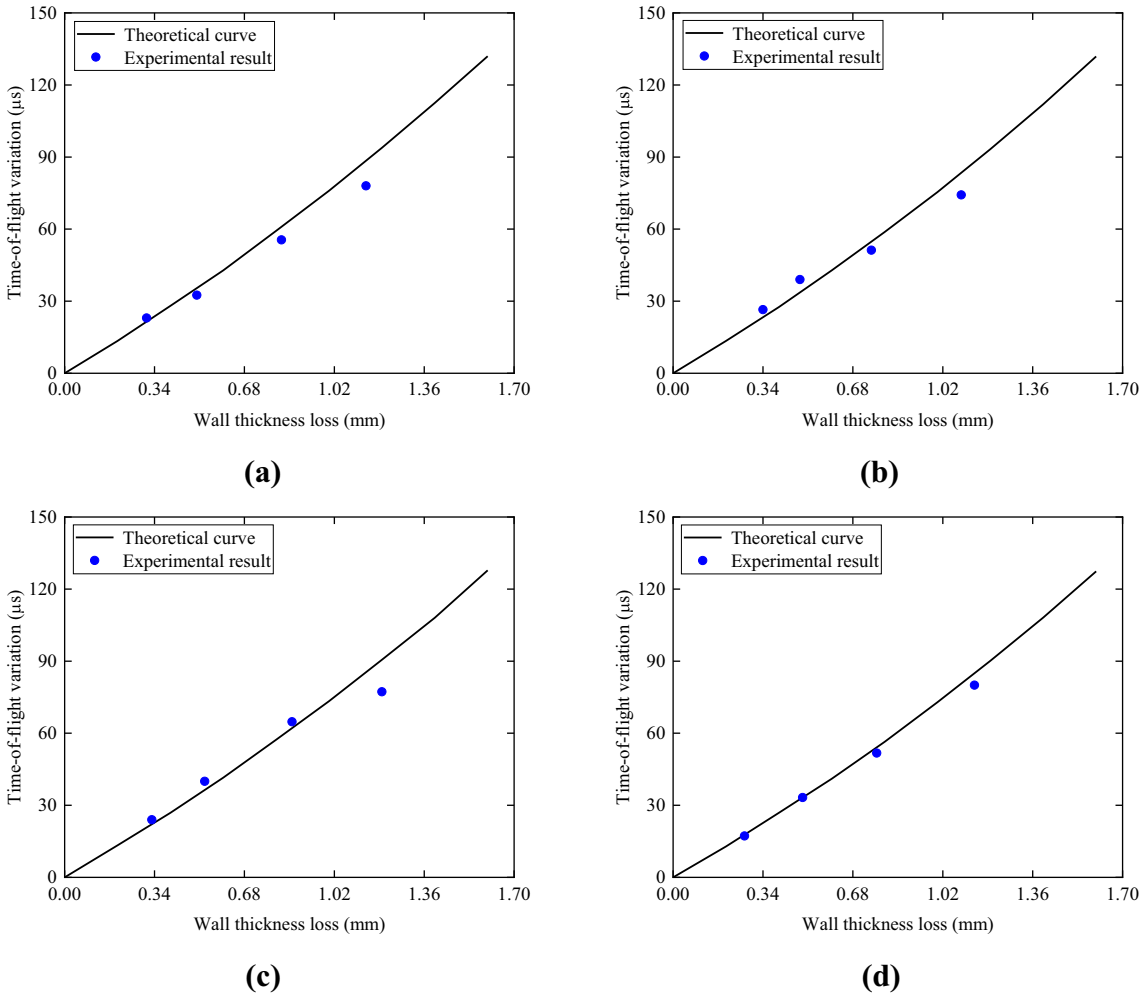

Fig. 15 Time-of-flight variations of the reflected waves with different wall thickness losses: **a** path1, **b** path2, **c** path3, and **d** path4

accumulated propagation length in a certain range can be further increased, and higher resolution and quantification precision for CIWTL can be obtained. The proposed methodology can effectively detect the CIWTL of a continuous pipe, and thus, the strength and integrity of the pipe can be comprehensively evaluated, and the remaining service life of the pipe can be effectively predicted. This methodology is simple and cost-efficient and can provide distributed monitoring. The corrosion of long-distance pipes can be quantitatively detected in a fast and comprehensive way using only a few permanent detection points. In contrast, point-by-point UT is inefficient, unable to detect physically inaccessible regions, and cannot comprehensively and quantitatively detect the CIWTL of long-distance pipes in a continuously distributed manner. Moreover, its detection precision is affected by various factors, such as coupling effect. The proposed methodology makes up for these drawbacks of the conventional UT.

5 Conclusions

In this study, an innovative CIWTL detection methodology based on the reflected L(0,1) guided wave in continuous pipes was proposed. A theoretical analysis showed that increasing the accumulated propagation length of the L(0,1) guided wave improved its sensitivity to CIWTL in the selected dispersion range. The reflected L(0,1) guided wave, which had a longer accumulated propagation length in a certain range, was generated by making discontinuities on both sides of local pipe section within a continuous pipe. The TOF variation of the reflected L(0,1) guided wave was proposed as a CIWTL-sensitive feature to identify the CIWTL of the pipe section. Furthermore, the quantitative relationship between the TOF variation of the reflected wave and CIWTL was established theoretically and used to quantify the CIWTL of the pipe section. The increase in accumulated propagation length enabled high-resolution measurement of the CIWTL. Then, the

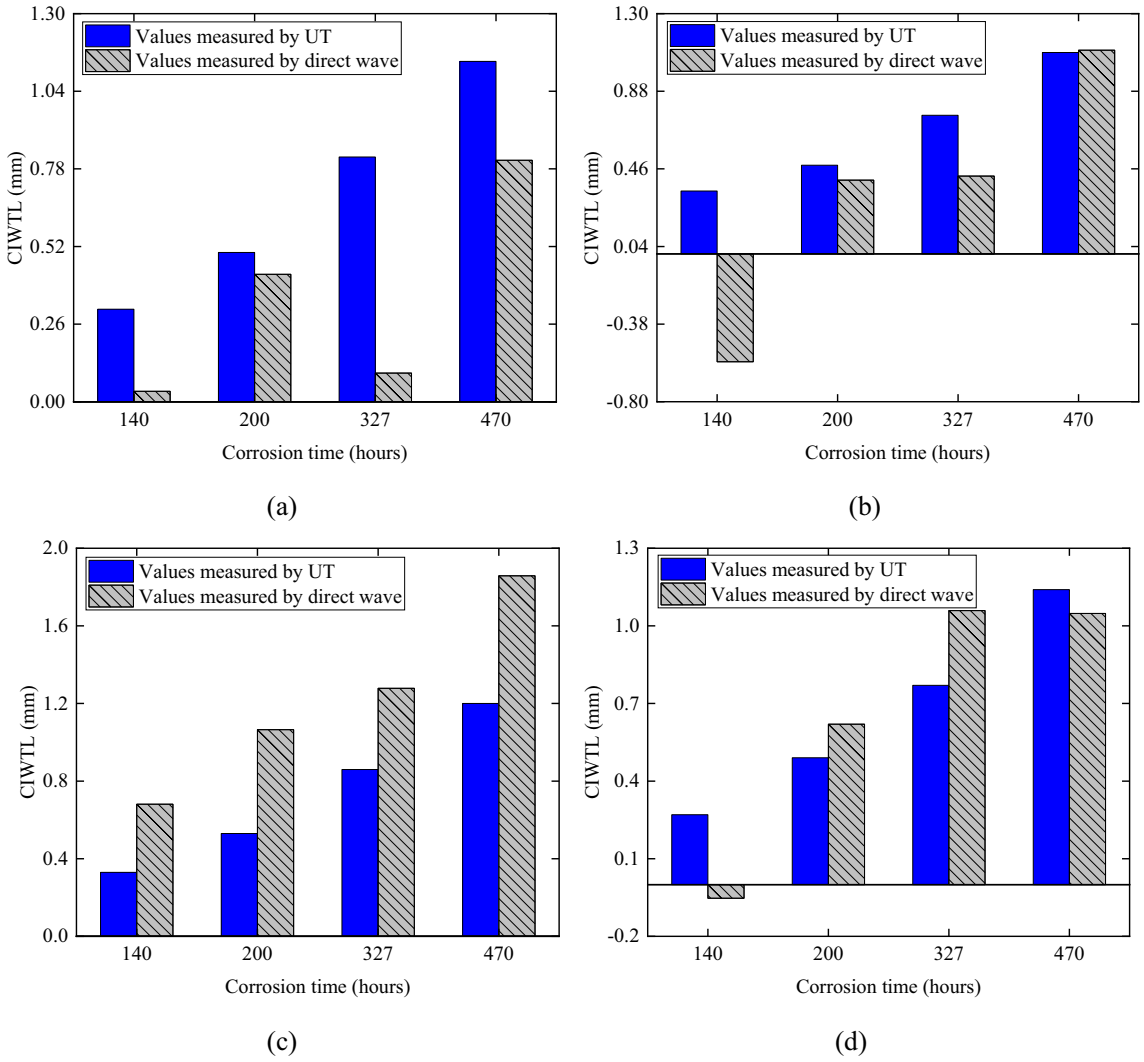

Fig. 16 CIWTLs measured by the TOF variations of the direct waves and UT: **a** path1, **b** path2, **c** path3, and **d** path4

proposed methodology could be used to detect the CIWTL of the next pipe section and extended to detect the CIWTL of a continuous pipe in a large-scale and distributed manner. The effectiveness of this methodology was demonstrated through an experiment. The experimental results indicated that the reflected L(0,1) mode was generated by artificial discontinuities, and this methodology effectively detected the CIWTL of the pipe. The TOF variation of the reflected wave was sensitive to minor wall thickness loss, and a small wall thickness loss of 0.27 mm was quantified. Compared with the TOF variation of the direct wave, this methodology improved the resolution of CIWTL measurement. During the whole corrosion process, the TOF variation of the reflected wave increased as the CIWTL increased, and the TOF variations of the reflected waves were consistent with the corresponding theoretical TOF variations. This methodology had a large detection range for the CIWTL and could effectively detect values of the CIWTL exceeding 15% of the initial wall thickness. The CIWTL of the pipe was accurately quantified using the proposed methodology. The relative errors between the values measured by the proposed method and those measured by UT were small; the maximum relative error was -11.93%. The CIWTLs of different paths of the pipe were effectively estimated through the deployed receiver network. The proposed methodology has higher resolution and quantification precision for CIWTL than current GWB methods. Additionally, this methodology has high efficiency and anti-interference and can quantitatively detect corrosion in a continuous pipe in a distributed manner, which overcomes the weaknesses of conventional pointwise NDT methods such as UT. Notably, this proposed methodology has only been proven to quantitatively detect CIWTL in pipes. For the effective detection of localized

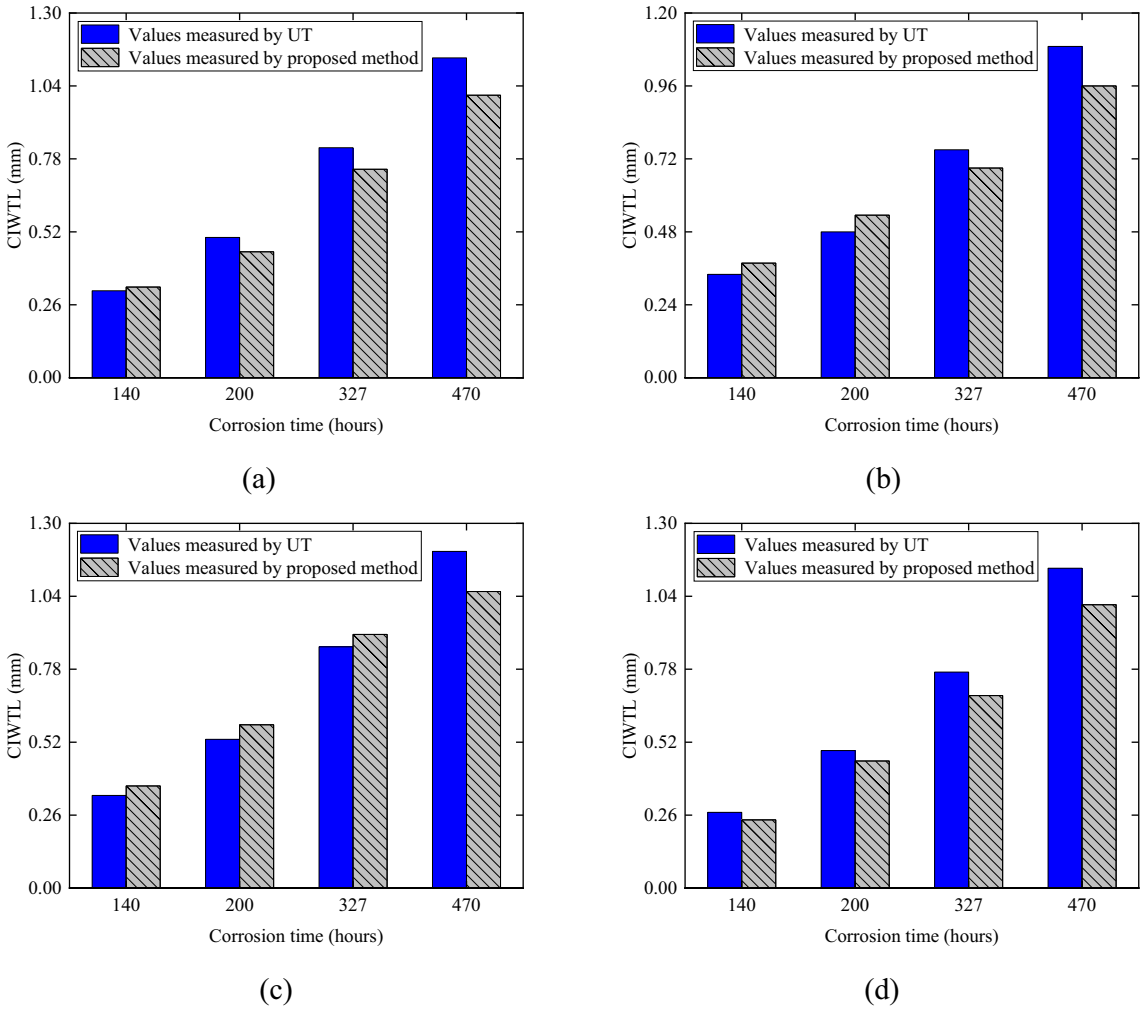

Fig. 17 CIWTLs measured by the proposed method and UT: **a** path1, **b** path2, **c** path3, and **d** path4

corrosion of a pipe, it will be necessary to further study the interaction mechanism of guided waves and localized defects, and high-performance signal processing techniques.

Acknowledgements This work was supported by the National Key R & D Program of China (Grant No. 2022YFC3801000) and the National Natural Science Foundation of China (Grant No. 52079024).

Data availability Data will be available upon reasonable request.

References

1. Li MH, Feng X (2022) Multisensor data fusion-based structural health monitoring for buried metallic pipelines under complicated stress states. J Civil Struct Health Monit. 21:1–13
2. Li MH, Feng X, Han Y (2022) Brillouin fiber optic sensors and mobile augmented reality-based digital twins for quantitative safety assessment of underground pipelines. Automat Constr 144:104617
3. Li MH, Feng X, Han Y, Liu XD (2023) Mobile augmented reality-based visualization framework for lifecycle O&M support of urban underground pipe networks. Tunn Undergr Sp Tech 136:105069
4. Ahmad Z (2006) Principles of corrosion engineering and corrosion control. Butterworth-Heinemann, London
5. Cicek V (2014) Corrosion engineering. Wiley, New York
6. Wu KY, Mosleh A (2019) Effect of temporal variability of operating parameters in corrosion modelling for natural gas pipelines subject to uniform corrosion. J Nat Gas Sci Eng 69:102930
7. Yeshanew DA, Jiru MG, Ahmed GMS, Badruddin IA, Soudagar MEM, Kamangar S, Tolcha MA (2021) Corrosion characterization at surface and subsurface of iron-based buried water pipelines. Materials 14(19):5877
8. Krautkrämer J, Krautkrämer H (1990) Ultrasonic testing of materials. Springer, Berlin
9. Lei H, Huang Z, Liang W, Mao Y, Que PW (2009) Ultrasonic pig for submarine oil pipeline corrosion inspection. Russ J Nondestruct 45(4):285–291
10. Rodríguez-Olivares NA, Cruz-Cruz JV, Gómez-Hernández A, Hernández-Alvarado R, Nava-Balanzar L, Salgado-Jiménez T, Soto-Cajiga JA (2018) Improvement of ultrasonic pulse generator for automatic pipeline inspection. Sensors 18(9):2950

11. Nguyen L, Miro JV (2020) Efficient evaluation of remaining wall thickness in corroded water pipes using pulsed eddy current data. IEEE Sens J 20(23):14465–14473
12. Usarek Z, Warnke K (2017) Inspection of gas pipelines using magnetic flux leakage technology. Adv Mater Sci 17(3):37–45
13. Silva W, Lopes R, Zscherpel U, Meinel D, Ewert U (2021) X-ray imaging techniques for inspection of composite pipelines. Micron 2:103033
14. Ding XY, Xu CB, Deng MX, Zhao YX, Bi XY, Hu N (2021) Experimental investigation of the surface corrosion damage in plates based on nonlinear Lamb wave methods. NDT&E Int 121:102466
15. Rao J, Ratassepp M, Lisevych D, Caffoor MH, Fan Z (2017) Online corrosion monitoring of plate structures based on guided wave tomography using piezoelectric sensors. Sensors 17(12):2882
16. Zima B, Kędra R (2019) Reference-free determination of debonding length in reinforced concrete beams using guided wave propagation. Constr Build Mater 207:291–303
17. Tu JQ, Tang ZF, Yun CB, Wu JJ, Xu X (2021) Guided wave-based damage assessment on welded steel I-beam under ambient temperature variations. Struct Control Hlth 28(4):2696
18. Sriramadasu RC, Banerjee S, Lu Y (2019) Detection and assessment of pitting corrosion in rebars using scattering of ultrasonic guided waves. NDT&E Int 101:53–61
19. Amjad U, Yadav SK, Kundu T (2015) Detection and quantification of diameter reduction due to corrosion in reinforcing steel bars. Struct Health Monit 14(5):532–543
20. Cawley P, Lowe MJS, Simonetti F, Chevalier C, Roosenbrand AG (2002) The variation of the reflection coefficient of extensional guided waves in pipes from defects as a function of defect depth, axial extent, circumferential extent and frequency. P I Mech Eng C-J Mec 216(11):1131–1143
21. Nurmalia, Nakamura N, Ogi H, Hirao M (2017) EMAT pipe inspection technique using higher mode torsional guided wave T(0,2). NDT&E Int 87:78–84
22. Li ZM, He CF, Liu ZH, Wu B (2019) Quantitative detection of lamination defect in thin-walled metallic pipe by using circumferential Lamb waves based on wavenumber analysis method. NDT&E Int 102:56–67
23. Livadiotis S, Ebrahimkhanlou A, Salamone S (2020) Monitoring internal corrosion in steel pipelines: a two-step helical guided wave approach for localization and quantification. Struct Health Monit 147:5921720970139
24. Demma A, Cawley P, Lowe M, Roosenbrand AG, Pavlakovic B (2004) The reflection of guided waves from notches in pipes: a guide for interpreting corrosion measurements. NDT&E Int 37(3):167–180
25. Carandente R, Ma J, Cawley P (2010) The scattering of the fundamental torsional mode from axi-symmetric defects with varying depth profile in pipes. J Acoust Soc Am 127(6):3440–3448
26. Løvstad A, Cawley P (2012) The reflection of the fundamental torsional mode from pit clusters in pipes. NDT&E Int 46:83–93
27. Zhu C, Xu ZD, Lu HF, Lu Y (2022) Evaluation of cross-sectional deformation in pipes using reflection of fundamental guided-waves. J Eng Mech 148(5):04022016
28. Park J, Lee J, Jeong SG, Cho Y (2019) A study on guided wave propagation in a long distance curved pipe. J Mech Sci Technol 33(9):4111–4117
29. Lowe MJS, Alleyne DN, Cawley P (1998) Defect detection in pipes using guided waves. Ultrasonics 36:147–154
30. Carandente R, Cawley P (2012) The effect of complex defect profiles on the reflection of the fundamental torsional mode in pipes. NDT&E Int 46:41–47
31. Wang XJ, Gao HM, Zhao K, Wang C (2021) Time-frequency characteristics of longitudinal modes in symmetric mode conversion for defect characterization in guided waves-based pipeline inspection. NDT&E Int 122:102490
32. Ennaceur C, Mudge P, Bridge B, Kayous M, Gan TH (2007) Application of the time reversal technique to the focusing of long-range ultrasound in pipelines. Insight-Non-Destruct Test Condition Monitor 49(4):217–223
33. Amjad U, Yadav SK, Kundu T (2015) Detection and quantification of pipe damage from change in time of flight and phase. Ultrasonics 62:223–236
34. Guan RQ, Lu Y, Wang K, Su ZQ (2019) Fatigue crack detection in pipes with multiple mode nonlinear guided waves. Struct Health Monit 18(1):180–192
35. Gazis DC (1959) Three-dimension investigation of the propagation of waves in hollow circular cylinders: I analytical foundation. J Acoust Soc Am 31(5):568–573
36. Rose JL (1999) Ultrasonic waves in solid media. Cambridge University Press, New York
37. Pavlakovic B, Lowe M, Alleyne D, Cawley P (1997) Disperse: a general purpose program for creating dispersion curves. In: Thompson DO, Chimenti DE (eds) Review of progress in quantitative nondestructive evaluation. Plenum Press, New York, pp 185–192
38. Engan HE (1998) Torsional wave scattering from a diameter step in a rod. J Acoust Soc Am 104(4):2015–2024
39. Demma A, Cawley P, Lowe M (2003) Scattering of the fundamental shear horizontal mode from steps and notches in plates. The J Acoust Soc Am 113(4):1880–1891
40. Ghavamian A, Mustapha F, Baharudin BTHT, Yidris N (2018) Detection, localisation and assessment of defects in pipes using guided wave techniques: a review. Sensors 18(12):4470
41. Alleyne DN, Cawley P (1996) The effect of discontinuities on the long-range propagation of Lamb waves in pipes. P I Mech Eng E-J Pro 210(3):217–226
42. Rioul O, Vetterli M (1991) Wavelets and signal processing. IEEE Signal Proc Mag 8(4):14–38